

Localized periodic patterns for the non-symmetric generalized Swift-Hohenberg equation

C. J. Budd¹, and R. Kuske²

¹Centre for Nonlinear Mechanics, University of Bath, UK, BA2 7AY

²Department of Mathematics, University of British Columbia, Canada V6T 1Z2.

Supported in part by NSF-DMS 0072311 and an NSERC Discovery Grant.

Corresponding author: rachel@math.ubc.ca, phone: (604) 822-4973, fax: (604)822-6074

Abstract

A new asymptotic multiple scale expansion is used to derive envelope equations for localized spatially periodic patterns in the context of the generalized Swift-Hohenberg equation. An analysis of this envelope equation results in parametric conditions for localized patterns. Furthermore, it yields corrections for wave number selection which are an order of magnitude larger for asymmetric nonlinearities than for the symmetric case. The analytical results are compared with numerical computations which demonstrate that the condition for localized patterns coincides with vanishing Hamiltonian and Lagrangian for periodic solutions. One striking feature of the choice of scaling parameters is that the derived condition for localized patterns agrees with the numerical results for a significant range of parameters which are an $O(1)$ distance from the bifurcation, thus providing a novel approach for studying these localized patterns.

Keywords: Asymptotic balance, Localized patterns, Lagrangian, Heteroclinic connection

1 Introduction

Spatially localized oscillatory patterns have been studied in a variety of models and contexts, including convection, chemical patterns, elasticity, and optics (see [1]-[7] and references therein). In order to study the appearance of this phenomenon, simplified models, such as the Swift-Hohenberg equation have been used. The Swift-Hohenberg equation has also been used as a canonical model to study many other properties of pattern dynamics.

Heterogeneity is an obvious cause of localized oscillations, since a spatially varying medium can lead to spatially varying patterns, or patterns appearing only in localized regions of space; for example, see [8], [9] and [10]. Heterogeneity is not a necessary condition for such patterns; localized oscillations can also occur in homogeneous systems, where they have been referred to as stable coexisting patterns [11, 12, 13], or where pinned interfaces or grain boundaries between rolls and steady states have been studied [14, 15]. It is typically more difficult to identify parametrically the conditions for spatially localized patterns in the homogeneous case, since they can arise through different mechanisms, depending on the

application. A number of experimental and computational results [1, 2, 11, 12, 13, 16], and many others, have shown that these localized oscillations can occur in different systems of reaction-diffusion and Swift-Hohenberg models. They appear in parameter regions corresponding to subcritical bifurcations [11, 13, 16, 17] and bistability regions [1, 2, 12] and in the presence of both symmetric and asymmetric nonlinearities.

In this paper we look for spatially localized cellular (roll type) patterns in the context of the generalized Swift-Hohenberg (SH) equation

$$u_t = \mathcal{L}u + f(u) \equiv - \left(q_c^2 + \frac{\partial^2}{\partial x^2} \right)^2 u + ru + f(u) \quad (1.1)$$

$$f(u) = b_2u^2 + b_3u^3 + b_4u^4 + b_5u^5 + \dots \quad (1.2)$$

A typical pattern of this type is illustrated in Figure 1.1 and comprises a sequence of near identical cells close to $x = 0$ with rapid decay to zero as $|x| \rightarrow \infty$ in the final cell. In the equation (1.2) u plays the same role as the variable for temperature in convection problems or concentration in chemical reactions, and r plays the role of a control or bifurcation parameter with a critical value of $r = 0$. It is well known that the zero solution is stable to periodic perturbations for $r < 0$, and for $r > 0$ extended periodic solutions (rolls) are stable.

We describe localized oscillatory solutions of (1.1) by deriving an equation for the envelope or amplitude of the patterns. An asymptotic expansion for u that balances relative sizes of the linear and nonlinear effects is the basis for the construction of the amplitude equation, which provides conditions for the localized solutions in terms of the model parameters. In particular, we are able to construct heteroclinic connections between the steady (zero) state and oscillatory patterns. The parameter values at which these heteroclinic connections occur lie at the centre of the range of parameters at which we observe roll patterns with an arbitrary number of rolls. Then we have a description of the interface or grain boundary for the coexisting steady state and rolls. The conditions for these heteroclinic connections between zero and the oscillatory patterns can be written in terms of a relationship between the bifurcation parameter r and the coefficients b_j of the nonlinear term in (1.2) which takes the form

$$\varepsilon^2(r) = \frac{3 \nu^2(b_j, r)}{4 g(b_j, r)}. \quad (1.3)$$

Here, the parameters ε^2 , ν and g are obtained from the coefficients in the amplitude equation, and we omit their arguments in the remainder of the paper. The parameter $1/\varepsilon \gg 1$ represents the length scale of the slow evolution of the pattern and $\sqrt{\nu}$ the ratio between the amplitude scale and ε . The expression (1.3) represents a curve which lies in the center of a region for observing these localized patterns; the region can be described by including exponentially small corrections to the result (1.3), but we do not compute these in this paper. These are discussed further in Section 6 and in [14, 15, 18].

Much of the analysis of this paper is motivated by [18] which gives an asymptotic analysis of the steady state equation for a strut on a Winkler foundation

$$u_{\xi\xi\xi\xi} + \mathcal{P}u_{\xi\xi} + u + a_2u^2 + a_3u^3 + a_4u^4 + a_5u^5 + \dots = 0, \quad (1.4)$$

with the load \mathcal{P} as bifurcation parameter. In studies [7] and [18] of (1.4) and in our consideration of the generalized Swift-Hohenberg equation (1.1), the focus is on two

classes of nonlinearity. In terms of the coefficients b_j , the first is the general asymmetric nonlinearity,

$$b_2 \neq 0, \quad 0 > b_3 > -b_2^2 h(q_c), \quad (1.5)$$

where $h(q_c)$ is a smoothly varying positive function of q_c which is defined later (see 3.8). This nonlinearity has been considered computationally in other studies of localized oscillatory patterns in the Swift-Hohenberg equations [12]. The second is the symmetric nonlinearity,

$$b_2 = b_4 = 0, \quad b_3 > 0, \quad b_5 < 0, \quad (1.6)$$

which has the additional symmetry

$$f(-u) = -f(u).$$

The symmetric case has been analyzed in [15] and studied computationally in [11].

Localized behaviour, comprising cellular patterns, occurs in the limit $\nu \rightarrow 0$, where the respective definitions of ν in the asymmetric and symmetric cases are

$$\nu = \frac{3}{2}[b_3 + b_2^2 h(q_c)] \quad \text{and} \quad \nu = b_3 / \sqrt{|b_5|} \rightarrow 0. \quad (1.7)$$

In the context of the amplitude equation the limit $\nu \rightarrow 0$ corresponds to a balance of the destabilizing and stabilizing nonlinear effects on the oscillations. In Figure 1.1 we show representative localized patterns of coexisting rolls and steady states for the different cases of symmetric and asymmetric nonlinearities, constructed from the asymptotic approximations for u .

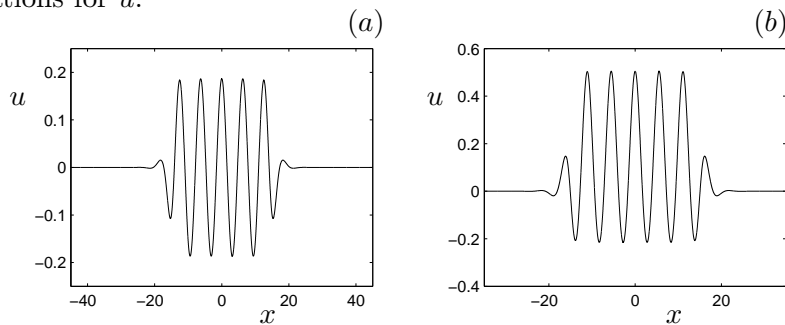


Figure 1.1: Representative graphs of localized cellular patterns for (a) the symmetric nonlinearity $b_2 = b_4 = 0$, and (b) the asymmetric nonlinearity $b_2 \neq 0$, both with $r < 0$.

In Figure 1.2 we show the condition (1.3) in terms of the parameters r and b_j for these localized roll solutions. The symmetric case given by (1.6) is somewhat easier to analyse as it admits symmetric solutions with zero mean and for which $u(x) = -u(x_0 - x)$ for some x_0 . We outline the general derivation for the general case (1.5) in the Sections 2 and 3. In the following Sections we show that there is a significant difference between the cases for symmetric $b_2 = b_4 = 0$ and asymmetric $b_2 \neq 0$ nonlinearities. The asymptotic results are compared with numerics for both cases.

The main ingredient of the construction is a crucial scaling of parameters that leads to an asymptotic expansion that balances relative sizes of the linear and nonlinear effects. This balance is the key to finding the parametric condition (1.3) for the localized cellular patterns shown in Figure 1.1. In contrast, previous analyses such as [12] and [15] rely on a close tie to the bifurcation parameter and the linearized problem about the critical

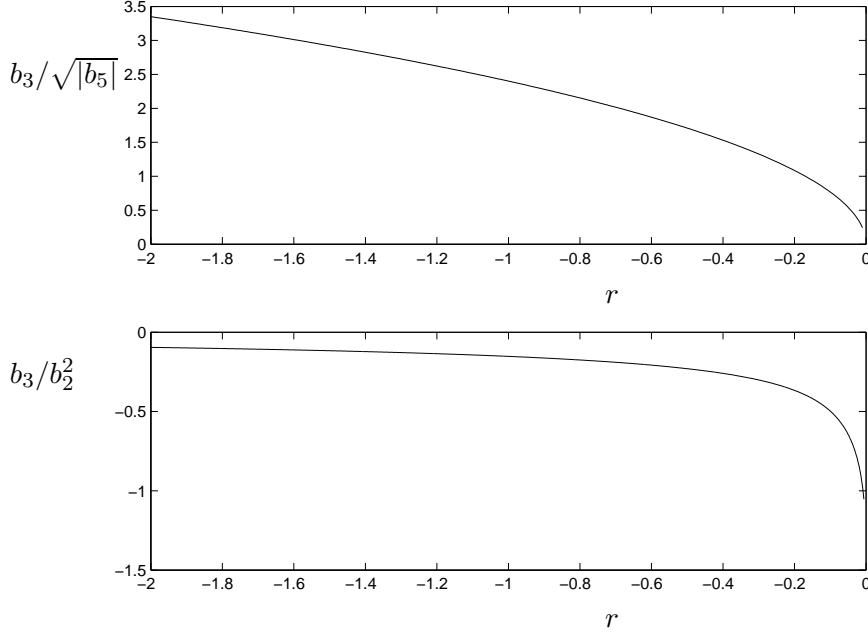


Figure 1.2: The asymptotic relationship (1.3) between r and the coefficients b_j of the nonlinear terms in $f(u)$ which corresponds to localized oscillatory solutions with an arbitrary number of cells, as predicted by the analysis. In the top graph we show the results for the symmetric nonlinearity r vs. $b_3/\sqrt{|b_5|}$, and in the bottom graph we show the results for the asymmetric nonlinearity r vs. b_3/b_2^2 . Note that we give the results for r an $O(1)$ distance from the critical value $r = 0$. In Section 4 we show the agreement with the results presented in this figure and the numerical calculations.

point $r = 0$. As we show in Sections 2 and 4, an approach of this type gives results which are valid in general only for parameter values very close to the bifurcation point $r = 0$. The analysis presented here is more flexible, and we show that it is valid well for parameter values an $O(1)$ distance from the bifurcation point. In Section 4 we compare our analytical results with previous results and numerical results, demonstrating the validity of the results for the range of r shown in Figure 1.2.

Our analysis also highlights a number of important properties of these localized oscillatory solutions. We show that the parametric condition (1.3) for localized rolls is equivalent to finding a periodic solution with vanishing Lagrangian L and Hamiltonian H for (1.1), with *Lagrangian integral* L (taken over one period) given by

$$L \equiv \int \left[-\frac{(u'')^2}{2} + 2q_c^2 \frac{(u')^2}{2} - (q_c^4 - r) \frac{u^2}{2} + F(u) \right] dx = 0, \quad \text{and} \quad F'(u) = f(u). \quad (1.8)$$

and the first integral, the *Hamiltonian* H , defined by

$$H = u'''u' - \frac{u''^2}{2} + 2q_c^2 \frac{u'^2}{2} + (q_c^4 - r) \frac{u^2}{2} + F(u). \quad (1.9)$$

The analysis of the amplitude equation also leads to phase corrections and asymptotic results for the wave number selection of the pattern. There have been a number of previous studies of the Swift-Hohenberg equation which have been concerned with amplitude equations, vanishing L and H , phase corrections, and wave number selection for localized

patterns. We give a careful accounting and comparison of the relevant results in the next section.

The remainder of this paper is organized as follows: In the next section we outline the main results and discuss their relationship with previous work. In Section 3 we derive the amplitude equation, give the analysis leading to the main analytical results, and also give the stability analysis using the amplitude equation. In Section 4 we compare the analytical results with computational results. In Sections 5 we demonstrate extensions to localized patterns with connections to non-zero steady states.

2 Main results and relationship with previous work

Several analyses have pointed towards the description of localized oscillations with amplitude equations in certain limits. Studies by Pomeau [19] Bensimon [14], Nepomnyaschy [15] and Sakaguchi and Brand [11] provide a general outline for looking for conditions for these localized patterns for specific nonlinearities in the Swift-Hohenberg equation, in terms of particular relative scalings between the bifurcation parameter, length scales, and the amplitude. These studies recognized some of the ingredients that were necessary for constructing these solutions, for example, nonlinearities in the amplitude equation which include quintic terms and particular scaling behavior of the bifurcation parameter. However, these previous results did not provide a way to map out these localized cellular patterns in parameter space or to construct these solutions for general nonlinearities.

We emphasize in this paper that the correct balance with nonlinear terms is crucial, leading to a flexibility in the results which are valid even for $O(1)$ values of $|r|$. First we outline the difference in the approach for deriving the amplitude equation. Then we also compare other results related to the Lagrangian L , the Hamiltonian H , and wave number selection.

2.1 Overview and description of the amplitude equation

The key feature of the analysis is a description of the behaviour of the solution which is valid both close to the bifurcation point $r = 0$ and for values an $O(1)$ distance from $r = 0$. We achieve this by considering an expansion which involves three small parameters which have a subtle interaction. In particular, we look for steady state solutions which have a slow *spatial scale* $X = \varepsilon x$ and an *amplitude scale* δ with $\varepsilon \ll 1, \delta \ll 1$. The asymptotic approximation of the stationary solution for u is given by

$$u(x) \equiv u(x, X) \sim \delta u_1(x, X) + \delta^2 u_2(x, X) + \delta^3 u_3(x, X) + \dots \quad (2.1)$$

The scales δ and ε are related via the expression

$$\delta = \varepsilon/\nu^{1/2}, \quad (2.2)$$

where $\varepsilon \ll 1$ is closely related to r and ν depends on the values of b_j . We define ε presently, and here note that ν , defined in (1.7) can vary in order of magnitude from $O(1)$ to $O(\varepsilon)$. Then δ can vary in scale between ε and $\sqrt{\varepsilon}$ and the expansion (2.1) is valid over

a significant range of values of r . We now describe the differences between this approach and that of previous asymptotic approximations and associated amplitude equations.

The usual derivation via perturbation theory of the amplitude equation for extended cellular patterns or rolls in the Swift-Hohenberg equation is described for example in [20]. In summary, near the critical value $r = 0$, a small parameter $\tilde{\varepsilon} \ll 1$ is chosen so that

$$\tilde{\varepsilon}^2 = -r > 0, \quad (2.3)$$

for the subcritical case, and a slow spatial variable $\tilde{X} = \tilde{\varepsilon}x$ is also defined. Then a standard multiple scales asymptotic expansion for u is given in the generic form [20]

$$u(x) \sim \tilde{\varepsilon}U_1(x, \tilde{X}) + \tilde{\varepsilon}^2U_2(x, \tilde{X}) + \tilde{\varepsilon}^3U_3(x, \tilde{X}) + \dots, \quad (2.4)$$

which is equivalent to taking $\nu = 1$ in (2.2). More precisely, the stationary solution u is a slowly varying modulation of a more rapidly varying spatial oscillation taking the following form for the stationary case

$$u(x) \sim \tilde{\varepsilon}\tilde{A}_1(\tilde{X})e^{ikx} + \text{c.c.} + \tilde{\varepsilon}^2 \left[\tilde{A}_0(\tilde{X}) + \tilde{A}_2(\tilde{X})e^{2ikx} + \text{c.c.} \right] + \mathcal{O}(\tilde{\varepsilon}^3) \dots \quad (2.5)$$

In the usual derivation, k is taken to be the critical wave number $k = q_c$ corresponding to the most rapidly growing mode of the solution of the linearised equation at $r = 0$. Then an equation for the amplitude $\tilde{A}_1(\tilde{X})$ as a function of the slow variable \tilde{X} is derived using the method of multiple scales and perturbation analysis [20]. For the scaling given in (2.5) we get a stationary equation for $\tilde{A}_1(\tilde{X})$ of the following Ginzburg-Landau form,

$$(6k^2 - 2q_c^2)\tilde{A}_1\tilde{X}_{\tilde{X}} = \tilde{A}_1 - 2\tilde{\nu}|\tilde{A}_1|^2\tilde{A}_1, \quad (2.6)$$

where $\tilde{\nu}$ is a constant related to the parameters of the original equation which approaches ν (1.7) as $r \rightarrow 0$. Solving (2.6), we get an expression for $\tilde{\varepsilon}\tilde{A}_1(\tilde{X})$ which describes a small amplitude homoclinic solution for A [21],

$$\tilde{\varepsilon}\tilde{A}_1(\tilde{X}) = \frac{\tilde{\varepsilon}}{\tilde{\nu}^{1/2}} \operatorname{sech} \left(\frac{\tilde{X}}{\sqrt{6k^2 - 2q_c^2}} \right) \quad \text{with} \quad \tilde{X} = \tilde{\varepsilon}x. \quad (2.7)$$

We see clearly that as $\tilde{\nu} \rightarrow 0$, the asymptotic validity of this solution is lost, so that the scaling used in (2.5) is incorrect. Indeed the breakdown is associated with the creation of the spatially localized oscillations, which have a different form. This motivates the choice of δ that we use in the more generally valid asymptotic expansion we construct presently. In terms of the amplitude equation, this breakdown corresponds to the case when an equation of the form (2.6) is not sufficient to describe the envelope of the localised solutions, and an alternative for the balance of leading order terms in the amplitude equation must be found. To do this we must include additional higher order terms in the amplitude equation to resolve the degeneracy related to $\tilde{\nu} \rightarrow 0$. That is, we look for a stationary equation with quintic nonlinearity, such as,

$$c_1\tilde{A}_{XX} = c_2\tilde{A} - 2c_3\tilde{A}^3 + c_4\tilde{A}^5 + ic_5\tilde{A}_X|\tilde{A}|^2. \quad (2.8)$$

One way to obtain an equation of this form from a multi-scale expansion, is to use a different amplitude scaling in which we take $\delta = \tilde{\varepsilon}^{1/2}$ so that $\nu = \tilde{\varepsilon}^{1/2}$ in (2.2). This leads to an expression for u of the following form

$$u \sim \tilde{\varepsilon}^{1/2}U_1(x, \tilde{X}) + \tilde{\varepsilon}U_2(x, \tilde{X}) + \tilde{\varepsilon}^{3/2}U_3(x, \tilde{X}) + \dots, \quad \tilde{X} = \tilde{\varepsilon}x, \quad (2.9)$$

where $\tilde{\varepsilon}$ is the same as in (2.4). An expansion of the solution in this form for the symmetric Swift-Hohenberg equation is described in [15]. Substituting as before, and expanding in powers of $\tilde{\varepsilon}$ yields a series of equations of the form:

$$\begin{aligned} O(\tilde{\varepsilon}^{1/2}) : \quad & \left(\frac{\partial^2}{\partial x^2} + q_c^2 \right)^2 U_1 = 0 \\ O(\tilde{\varepsilon}^{j/2}) : \quad & \left(\frac{\partial^2}{\partial x^2} + q_c^2 \right)^2 U_j = H_j. \end{aligned} \quad (2.10)$$

for the stationary solution. Then $U_1 = \tilde{A}_1(\tilde{X})e^{ikx} + \text{c.c.}$ with $k = q_c$ as before, and H_j involves derivatives of $\tilde{A}(\tilde{X})$ and U_m for $m < j$. This yields an equation of the form (2.8) for \tilde{A}_1 , with $c_5 = 0$ for the case of the symmetric underlying equation. Whilst this analysis works well close to $r = 0$ it loses resolution for localized cellular oscillations as $|r|$ increases. In Section 3, following (3.3) we show how the equations in (2.10) resulting from the ansatz (2.9) restrict the validity of the higher order terms and coefficients in the amplitude equation to a neighborhood close to $r = 0$. The resulting loss of resolution for increasing $|r|$ is most significant when the underlying equation is not symmetric, corresponding to a lack of conservation of the angular momentum in the envelope equation. We see this loss of resolution in the comparison with numerical experiments presented in Section 4.

To overcome these problems, we now present an analysis for which we define a different expansion for u of the general form (2.1). Here the ideas from (2.4) and (2.9) are combined to yield a more general amplitude scaling. More precisely, we again consider a slowly modulated oscillating solution of the form

$$u(x) \sim \delta A_1(X)e^{ikx} + \text{c.c.} + \delta^2 [A_0(X) + A_2(X)e^{2ikx} + \text{c.c.}] + \mathcal{O}(\delta^3) \dots \quad (2.11)$$

We take

$$\delta = \varepsilon/\nu^{1/2}$$

with ν given in (1.7) and $X = \varepsilon x$, replacing the definition of $\tilde{\varepsilon}$ with

$$\varepsilon^2 = (q_c^2 - k^2)^2 - r \equiv \mu_1(k). \quad (2.12)$$

This definition of ε includes an additional dependency on q_c and k which allows us to consider $O(1)$ values of $|r|$. This definition follows from a consideration of the amplitude equation, balancing the linear and the nonlinear terms. The spatial scaling parameter ε is defined in terms of the symbol of the linear operator \mathcal{L}

$$\mathcal{L}e^{imkx} = (q_c^2 - m^2k^2)^2 - r \equiv \mu_m(k). \quad (2.13)$$

The function μ_m appears again in the analysis of the next section, and k is determined as part of the analysis. When k is close to q_c this definition of ε in (2.12) is close to that of $\tilde{\varepsilon}$. However, as shown above, the scalings in (2.5) lead to an amplitude equation (2.6) which is not appropriate for describing localized rolls, so we must use a different scaling for the amplitude.

With this choice of parameters in the expansion, we expand in powers of δ and find a series of equations of the form

$$O(\delta) : \quad \left(\frac{\partial^2}{\partial x^2} + q_c^2 \right)^2 U_1 - rU_1 = 0$$

$$O(\delta^j) : \quad \left(\frac{\partial^2}{\partial x^2} + q_c^2 \right)^2 U_j - rU_j = H_j, \quad (2.14)$$

as shown in detail in Section 3. The definition of ν (1.7) is obtained through this expansion as the coefficient of the cubic nonlinearities. By balancing the linear, cubic, and quintic nonlinearities for the amplitude A , this expansion avoids the breakdown of (2.6), and we get

$$(6k^2 - 2q_c^2) \frac{\varepsilon^2}{\delta^4} A_{1XX} = \frac{\varepsilon^2}{\delta^4} A_1 - 2 \frac{\nu}{\delta^2} |A_1|^2 A_1 + c |A_1|^4 A_1 + i \frac{\varepsilon}{\delta^2} d A_{1X} |A_1|^2, \quad (2.15)$$

where c and d are derived parameters which depend on b_j and r , as given in the Appendix. The amplitude equation (2.15) has non-zero fixed points corresponding to periodic solutions of the Swift-Hohenberg equation. The balance of all terms in (2.15) corresponds to small values of $\nu = O(\varepsilon)$, so that $\delta = O(\varepsilon^{1/2})$. The expansion (2.11) combined with the definition of ε (2.12) yields a derivation which is not closely tied to $r = 0$, but rather is based on a balance of linear and nonlinear terms for a larger range of parameter values, including $r = O(1)$. The form of (2.14) in which r appears, contrasted with (2.10), gives evidence of this difference, and we give further details in Section 3. As $r \rightarrow 0$ the scaling of the amplitude in (2.11) is similar to (2.9), and not to (2.5). As $|r|$ increases away from 0, the balance of terms in (2.15) is due to the form of the parameters δ and ε .

When looking for steady solutions $A(X) = \rho(X)e^{i\varphi(X)}$ from (2.15) we find a heteroclinic connection between the origin and one of the fixed points of the amplitude equation which describes the spatially localized oscillations of the Swift-Hohenberg equation which arise as heteroclinic connections between the zero solution and a periodic solution. In terms of ρ this connection takes the form

$$\delta\rho(X) = \sqrt{\frac{3}{g}} \frac{\varepsilon^{1/2}}{\sqrt{1 + e^{\theta X}}} \quad \text{with} \quad \theta = \sqrt{\frac{2}{3k^2 - q_c^2}}, \quad (2.16)$$

with g in terms of c and d (3.16). The condition for such a connection is given by

$$\varepsilon^2 = \frac{3\nu^2}{4g}, \quad (2.17)$$

as indicated in (2.2). This is a key result of the paper, as it gives the link between r and b_j for the system to have an arbitrarily large number of localized rolls. (In fact we see such an arbitrarily large number over an interval of values, the width of which decreases exponentially as $r \rightarrow 0$ [18].) Since the heteroclinic connection for the amplitude equation corresponds to localization of the oscillations, the condition (2.17) gives the critical condition for localized cellular patterns. The same condition holds in the asymmetric case, and in that case we also get a phase correction through determining φ . In Section 4 we calculate the corresponding periodic solution of the Swift-Hohenberg equation which is the limit of the heteroclinic connection.

Since (2.11) and (2.9) both lead to amplitude equations of the same form, (2.15) and (2.8), respectively, a condition for heteroclinic connections similar to (2.17) can also be obtained from (2.8). The condition corresponding to the expansion (2.9) was given in [15] for the symmetric case ($b_2 = b_4 = 0$), and it can be also be obtained by taking the limit as $r \rightarrow 0$

in the coefficients ν and g in (2.17). However, for r not very close to zero, the results from the two expansions are different. A comparison of the derivation of the equations (2.15) and (2.8) explains why this is so. The expansion (2.9), equivalent to the approach used in [15], scales the amplitude with $|r|^{1/4}$ for $|r| \ll 1$. Then the parameter r does not appear in the linear operator on the left hand side of (2.10), and as a consequence, r does not appear in the coefficients of the nonlinear terms in the amplitude equation (2.8). In contrast, using (2.11) yields a linear operator as given in (2.14) in which r does appear, since δ rather than r is assumed to be small. Then r is included in the expressions for u_j and consequently also in the coefficients ν and g . The scaling of the amplitude with δ rather than r , and the subsequent balancing of linear and nonlinear terms using the expressions for ε and ν , provides an expansion based on a combination of parameters rather than a single parameter. Then the expansion (2.11) yields results valid for a larger range of r , while expansions based on (2.9) correspond to values of r quite close to zero, particularly for the general asymmetric case of $b_2 \neq 0$.

By introducing the parameter δ as the size of the amplitude, we allow a solution which describes the behavior over a larger range of parameters. The amplitude is related not just to ε , but also to ν . The significance of the parameter ν is that it is small for parameters in which there is a localized oscillatory pattern, that is, a heteroclinic connection in the amplitude equation. The amplitude is not tied strictly to ε , but it can also vary with ν , so that different types of solutions can be approximated using (2.11). Note that one can use the expansion (2.11) to obtain solutions of the form (2.7) for parameter ranges corresponding to $\nu = O(1)$, since the leading order equation (2.6) is recovered from (2.8) in this range. Thus the expansion (2.11) can be used to describe small homoclinic solutions for $\nu = O(1)$ and localized cellular patterns described by heteroclinic connections from the origin to the periodic solution for $\nu \ll 1$.

In the context of the amplitude equation, we note some significant differences between the symmetric and asymmetric cases. In [15] an approximation for the envelope equation was constructed, using an analysis about $r = 0$. In the symmetric case this construction is relatively straightforward, since higher harmonics do not play a significant role in the construction of the solution. Using the symmetry, it is possible to infer the form of the equation for the amplitude A of the primary mode of the oscillatory behavior $u \sim Ae^{ikx}$ for $k = q_c$. However, as we show in Section 3, in the asymmetric case it is essential to do a careful balance between nonlinear and linear terms, since secondary modes play a significant role in the construction of the amplitude equation. Furthermore, through this analysis we show that in the symmetric case there is technically a correction to the asymptotic behavior obtained in [15], but in practice this correction is very small, so that the analysis of [15] gives a good result. This is shown in detail in Section 3. In [18] it was shown that this correction has a larger effect on the condition for the heteroclinic for a strut with symmetric nonlinearity. There the results are in terms of a different bifurcation parameter, the load \mathcal{P} , which is the coefficient of the second derivative term.

2.2 Wave number selection and L and H

We also consider the important conditions that both the Lagrangian L (1.8) and Hamiltonian H (1.9) vanish for a periodic solution, equivalent to the condition (2.17). In [15] these conditions were found for the symmetric case $b_2 = b_4 = 0$. They are

necessary conditions for the heteroclinic connections underlying the localized patterns, or in the terminology of [15], the pinning of a grain boundary between coexisting periodic and uniform steady states. In Section 4 we consider periodic solutions for which $H = 0$ and $L = 0$. We compute these solutions numerically, and see the correspondence of the condition $L = H = 0$ with the wave number selection $k \approx q_c$. Through computations and in the analysis of the amplitude equation in Section 3, we see that the conditions $H = 0$ and $L = 0$ play a prominent role in the construction of the localized solutions. These conditions hold for both the asymmetric and symmetric cases. The form of L and H for (1.1) is similar to that for the strut on a Winkler foundation (1.4). In [18] it was shown that the criteria $L = H = 0$ are equivalent to the equation for the Maxwell load $\mathcal{P} = \mathcal{P}_M$, the critical load for which localized buckling is observed.

Differences in the phase correction are also found when contrasting the asymmetric and symmetric cases. In [15] the phase correction in the wave number selection for the symmetric nonlinearity was given by

$$k = q_c + O(r^2). \quad (2.18)$$

Since this correction is very small for r near 0, an analysis which is based solely on the primary mode $e^{iq_c x}$ gives a good approximation. We confirm this using our analysis for the symmetric case. However, in the asymmetric case, the phase correction to $k = q_c$ in the localized behavior is $O(\nu) = O(\varepsilon)$, as also shown in the numerical calculations in Section 4. In Section 3.1 we give an explicit value for this phase correction (3.27), using the envelope equation and looking for heteroclinic connections from zero to periodic solutions. This difference in the phase correction is related to the following loss of symmetry of the envelope equation in the asymmetric case. In [15] it was observed for the symmetric case that solutions of the amplitude equation written as $A = \rho e^{i\varphi}$ are solutions for $\varphi = \text{constant}$. That is, from the envelope equation for A , it can be shown that the angular momentum $\rho^2 \varphi'$ vanishes, where $'$ denotes a spatial derivative. In contrast, in the asymmetric case, the envelope equation no longer has vanishing angular momentum; rather $\rho^2 \varphi' + \mathcal{C} \rho^4 = 0$ for $\mathcal{C} = \text{constant}$, as shown in Section 3.1.

A number of other studies have explored the existence and dynamics of localized patterns by other methods. These types of solutions were obtained numerically in [12] for the SH equation and for other models in [1, 2] by looking for connections between steady states ($u = \text{constant}$) and stable roll solutions in bistable parameter regimes. In [17], the theory of dynamical systems was used to study the existence and stability properties of static localized structures, describing these patterns as fronts between homogeneous and periodic patterns. Their focus was on parameter regimes without bistability, such as in the subcritical regime where extended rolls are unstable, and computations were included to illustrate their description. In [11, 16, 22] these localized patterns were numerically explored further in subcritical regimes for the SH equation. In the next section we construct these solutions analytically for a general nonlinearity, and in Section 5 we extend this analysis to also give parameter regimes in which localized solutions exist due to connections between non-zero steady states and periodic oscillations about these steady states. These appear in parameter regimes in which these non-zero steady states are not stable.

3 The Amplitude Equation for localized solutions

In this section we outline the derivation of the amplitude equation, which leads to the condition for localized solutions. A similar calculation is given in [18], and we provide the details particular to this application here. We focus on stationary solutions in the general non-symmetric case when $b_2 \neq 0$. Essentially the same approach is used in the symmetric case $b_2 = b_4 = 0$, and is discussed in less detail in Section 3.2. Time-dependent behavior is considered in Section 3.3.

Starting with the generalized Swift-Hohenberg equation (1.1) we look for an equation for the slowly varying amplitude of the primary mode with frequency k . For stationary solutions, we then expand the function $u(x, X)$ in terms of the small parameter δ , as in (2.11). Then we replace $u'(x)$ by the compound expression $u'(x) = u_x + \varepsilon u_X$. Even though the two spatial scales are not independent, we treat them as independent in a multiple scales expansions. For clarity we mainly consider the case

$$\nu = \mathcal{O}(\varepsilon) \Rightarrow \delta = \mathcal{O}(\varepsilon^{1/2}), \quad (3.1)$$

anticipating that we are looking for the heteroclinic solution corresponding to localized solutions. From the derivatives we then get terms which have coefficients ε^j , which then are $\mathcal{O}(\delta^{2j})$ from (3.1). Once these scalings and expansions are chosen, the derivation of the amplitude equation is a straightforward envelope equation calculation.

We now substitute the expansion (2.11) into (1.1), and obtain a sequence of equations for $u_j(x, X)$, $j = 1 - 5$, by equating the coefficients of like powers of δ . These equations are of standard form

$$\mathcal{O}(\delta) : \quad \mathcal{L}u_1 = \left[\left(q_c^2 + \frac{\partial^2}{\partial x^2} \right)^2 - r \right] u_1 = 0 \quad (3.2)$$

$$\mathcal{O}(\delta^j) : \quad \mathcal{L}u_j = H_j(u_1, u_2, \dots, u_{j-1}), \quad j > 1. \quad (3.3)$$

Here H_j is function of the u_m , $m < j$, which have already been determined at lower order in δ . It includes derivatives with respect to both x and X , as well as terms without derivatives. Specifically, the sequence (3.3) is

$$\begin{aligned} \mathcal{O}(\delta^2) : \quad & \mathcal{L}u_2 = b_2 u_1^2 \\ \mathcal{O}(\delta^3) : \quad & \mathcal{L}u_3 = -4 \frac{\varepsilon}{\delta^2} (u_1)_{Xxxx} + 2b_2 u_1 u_2 - 4 \frac{\varepsilon}{\delta^2} q_c^2 (u_1)_{Xx} + 2b_2 u_1 u_2 + b_3 u_1^3 \\ \mathcal{O}(\delta^4) : \quad & \mathcal{L}u_4 = b_2 u_2^2 - 4 \frac{\varepsilon}{\delta^2} (u_2)_{Xxxx} - 4 \frac{\varepsilon}{\delta^2} q_c^2 (u_2)_{Xx} + 2b_2 u_1 u_3 + 3b_3 u_1^2 u_2 + b_4 u_1^4 \\ \mathcal{O}(\delta^5) : \quad & \mathcal{L}u_5 = -2 \frac{\varepsilon^2}{\delta^4} q_c^2 (u_1)_{XX} - 6 \frac{\varepsilon^2}{\delta^4} (u_1)_{XXxx} - 4 \frac{\varepsilon}{\delta^2} q_c^2 (u_3)_{Xx} - 4 \frac{\varepsilon}{\delta^2} (u_3)_{Xxxx} + 2b_2 u_2 u_3 \\ & + 4b_4 u_1^3 u_2 + b_5 u_1^5 + 2b_2 u_1 u_4 + 3b_3 (u_1^2 u_3 + u_1 u_2^2) \end{aligned} \quad (3.4)$$

As discussed in Section 2, the linear operator \mathcal{L} in the sequence (3.2)-(3.3) includes r , and thus differs from (2.10) which was obtained using the expansion (2.9). Using an expansion for $|r| \ll 1$ of (3.3) yields (2.10).

With the ansatz

$$u_1 = A_1(X) e^{ikx} + \text{c.c.},$$

the leading order equation at $O(\delta)$ is

$$((k^2 - q_c^2)^2 - r)A_1(X) \equiv \mu_1(k)A_1(X) = 0. \quad (3.5)$$

Here $\mu_1(k) = \varepsilon^2 = O(\delta^4)$ (2.12), so that this term gives a contribution at higher order ($O(\delta^5)$). Thus the $O(\delta)$ equation is simply the identity $0 = 0$. At this stage the wave number k is not determined, and follows from the solvability conditions at higher order.

Next we solve the $O(\delta^2)$ equation, which yields

$$u_2 = A_0(X) + B_2(X)e^{2ikx} + \text{c.c.},$$

where

$$B_2(X) = b_2 \frac{A_1^2(X)}{\mu_2(k)} \quad \text{and} \quad A_0(X) = 2b_2 \frac{|A_1(X)|^2}{\mu_0(k)}. \quad (3.6)$$

Next we consider the $O(\delta^3)$ terms. To prevent resonance and consequent growth in u_3 we must avoid secular terms by ensuring that the right hand side $H_3(u_1, u_2)$ is orthogonal to the homogeneous solution $e^{\pm ikx}$ of the linear problem $\mathcal{L}u = 0$. Although $\mathcal{L}e^{ikx} = \mu_1(k)e^{ikx} \neq 0$, it yields a right hand side which is $O(\delta^4)$ from (3.5), and therefore at this order we may treat it as being the homogeneous solution. The secular terms can then only be zero to this order if

$$-\frac{\varepsilon}{\delta^2}(-4ik^3 A_1'(X) + 4iq_c^2 k A_1'(X)) + 2b_2(B_2 A_1^* + A_0 A_1) + 3b_3 |A_1|^2 A_1 = 0. \quad (3.7)$$

Now from (3.6) and (1.7), the terms which do not involve derivatives of $A_1(X)$ are given by

$$\left[2b_2^2 (\mu_2^{-1} + 2\mu_0^{-1}) + 3b_3\right] |A_1|^2 A_1 = 3 \left[b_2^2 h(q_c) + b_3\right] |A_1|^2 A_1 = 2\nu |A_1|^2 A_1. \quad (3.8)$$

Then $2\nu > 0$ is the coefficient of the cubic term in the envelope equation, as discussed in Section 2. There we showed that the magnitude of this coefficient is crucial in determining the behavior of the envelope, which motivates the choice of ν that we have taken in this paper. As mentioned above, we consider the case when $\nu = O(\varepsilon)$, so this expression is $O(\delta^2)$ and does not play a role at $O(\delta^3)$.

Thus, balancing terms of the same order, the solvability condition reduces to

$$4ik A_1'(X)[-k^2 + q_c^2] = 0. \quad (3.9)$$

Therefore either $A'(X) = 0$, which corresponds to a periodic solution of (1.1), or if the solution is slowly varying (a homoclinic or heteroclinic solution) we must have

$$k^2 = q_c^2 \quad (3.10)$$

to this order of asymptotics. Later we demonstrate that we obtain a correction to the frequency which is consistent with the condition that the Lagrangian energy of the periodic solution is zero (see Section 4). Because of the special structure of the linear operator in the SH equation, the wave number obtained in this construction is the same to leading order as that obtained using an expansion about the bifurcation point as in (2.9). In the analysis of [18], where the model has a similar structure but has a different bifurcation

parameter, it was shown that wave number of the localized oscillations is not necessarily the same as that obtained using an expansion about the bifurcation point.

If the scaling in (3.1) does not hold, that is, if

$$\nu = b_2^2 \left(\mu_2^{-1} + 2\mu_0^{-1} \right) + 3b_3/2 = \mathcal{O}(1)$$

with respect to ε , the results then obtained correspond to the region of parameter space in which the orbits of interest are homoclinic and not heteroclinic connections. In this case, the expansion (2.11) leads to the same result as the standard expansion (2.5), so that the quintic terms can be treated as higher order terms in the amplitude equation, as discussed in the previous section (2.6)-(2.7).

Proceeding with the expansion, given (3.10) the solvability condition for u_3 is satisfied for functions $A_1(X)$ for which $A_1'(X)$ is non-zero. Solving the resulting equation for u_3 then gives

$$u_3 = C_3(X)e^{3ikx} + \text{c.c.} \quad \text{with} \quad \mu_3 C_3 = A_1^3(X) \left(\frac{2b_2^2}{\mu_2(k)} + b_3 \right). \quad (3.11)$$

The solvability condition is automatically satisfied for the $\mathcal{O}(\delta^4)$ equation for u_4 , and we have simply that

$$u_4 = R_4 + B_4 e^{2ikx} + D_4 e^{4ikx} + \text{c.c.}$$

where R_4 , B_4 and D_4 are all functions of A_1 . Expressions for the coefficients R_4 and B_4 , which are simply corrections to the terms A_0 and B_2 , are given in the Appendix. We do not give an expression for the term D_4 here since it plays no further role in the derivation of the amplitude equation (3.12) for A_1 .

At $\mathcal{O}(\delta^5)$ we obtain a solvability condition for u_5 , avoiding secular terms, very much as in the calculation at $\mathcal{O}(\delta^3)$. This leads immediately to an envelope equation for A_1 . After a bit of algebra, this takes the form

$$(6k^2 - 2q_c^2) \frac{\varepsilon^2}{\delta^4} A_1'' = \frac{\varepsilon^2}{\delta^4} A_1 - 2 \frac{\nu}{\delta^2} A_1 |A_1|^2 + i \frac{\varepsilon}{\delta^2} d |A_1|^2 A_1'(X) + c |A_1|^4 A_1. \quad (3.12)$$

The coefficients c and d are also given in the Appendix. If the nonlinearity is symmetric in $f(u)$ ($b_2 = b_4 = 0$), then $d = 0$. As discussed in Section 2, the form of the amplitude equation (3.12) is the same as (2.8) which can be obtained using expansion (2.9). However, the coefficients of these two equations differ if $r \neq 0$. Through the scaling of the amplitude with δ in (2.11) and the resulting form of the system of equations (3.3), the coefficients ν , ε , c and d all involve the parameter r . The equation (3.12) obtained from (2.11) rather than (2.9) consequently holds for a larger range of parameter values corresponding to a balance of the linear and non-linear terms valid for constructing the localized oscillations.

3.1 Analysis of the amplitude equation

In this section we consider the phase of the solution and the related angular momentum. Looking for solutions of the amplitude equation of the form

$$A_1(X) = \rho(X) e^{i\varphi(X)},$$

with $\rho(X)$ real, and taking the imaginary part yields

$$(6k^2 - 2q_c^2)(\rho^2 \varphi_X)_X - d \frac{\delta^2}{\varepsilon} \rho^3 \rho_X = 0. \quad (3.13)$$

Integrating (3.13), we have the invariant quantity for the amplitude equation, the perturbed angular momentum

$$(6k^2 - 2q_c^2)\rho^2 \varphi_X - d \frac{\delta^2}{\varepsilon} \rho^4 / 4 = M. \quad (3.14)$$

This is an invariant in addition to the Hamiltonian H . In the asymmetric case $d \neq 0$ the angular momentum given by $\rho^2 \varphi_X$ is no longer invariant in contrast to the symmetric case $d = 0$ [15]. As we are considering connections to the zero solution, we take $M = 0$. Then the equation for ρ is

$$(6k^2 - 2q_c^2) \frac{\varepsilon^2}{\delta^4} \rho_{XX} = \frac{\varepsilon^2}{\delta^4} \rho - 2 \frac{\nu}{\delta^2} \rho^3 + g \rho^5, \quad (3.15)$$

where

$$g = c - \frac{3d^2}{16(6k^2 - 2q_c^2)}. \quad (3.16)$$

Now we make use of the conservation laws (3.13)-(3.15) and the first integral of (3.15) to derive conditions for heteroclinic connections and the associated wave number selection for localized rolls [15].

In general, (3.15) has a fixed point at $\rho = 0$ and a homoclinic solution connecting $\rho = 0$ to itself. This orbit satisfies the identity obtained by integrating ρ_X times (3.15) which is given by

$$\frac{6k^2 - 2q_c^2}{2} \frac{\varepsilon^2}{\delta^4} \rho_X^2 = \frac{\varepsilon^2}{2\delta^4} \rho^2 - \frac{\nu}{2\delta^2} \rho^4 + \frac{g}{6} \rho^6. \quad (3.17)$$

Setting $\rho_X = 0$ in this expression we have that the maximum amplitude ρ_H of the homoclinic solution is given by

$$\rho_H^2 = \frac{3\nu}{2g\delta^2} \left[1 - \sqrt{1 - \frac{4g\varepsilon^2}{3\nu^2}} \right] \quad (3.18)$$

provided that $\varepsilon^2 < 3\nu^2/4g$.

The amplitude equation also has two non-zero fixed points ($\rho_{XX} = 0$) at points $\rho_0^\pm > 0$ satisfying the quartic equation

$$\left(\rho_0^\pm\right)^2 = \frac{\nu}{g\delta^2} \left[1 \pm \sqrt{1 - \frac{g\varepsilon^2}{\nu^2}} \right]. \quad (3.19)$$

Observe that these fixed points correspond to those periodic solutions of the underlying system with frequency $k^2 = q_c^2$ to leading order. It is not difficult to show that

$$\rho_0^- < \rho_H \leq \rho_0^+$$

with equality on the right hand side occurring precisely when

$$\varepsilon^2 = 3\nu^2/4g. \quad (3.20)$$

At this point there is a heteroclinic connection from $\rho = 0$ to the fixed point ρ_0^+ and for which

$$\rho_0^2 = \rho_H^2 = \frac{3\nu}{2g\delta^2}. \quad (3.21)$$

Using (2.12) and (1.7), the condition (3.20) can be written in terms of q_c and the original coefficients b_j of $f(u)$ (1.2),

$$\mu_1 g = \frac{3}{4}\nu^2 = \frac{3}{4} \left[\frac{3}{2}b_3 + b_2^2 (\mu_2^{-1} + 2\mu_0^{-1}) \right]^2. \quad (3.22)$$

This is the condition for the existence of a heteroclinic connection of frequency $k^2 = q_c^2$ to leading order. This heteroclinic solution has the form,

$$\delta\rho(X) = \frac{\varepsilon^{1/2}}{\gamma\sqrt{1+e^{\theta X}}} \quad \text{with} \quad \gamma = \sqrt{\frac{g}{3}} \quad \text{and} \quad \theta = \sqrt{\frac{2}{3k^2 - q_c^2}}. \quad (3.23)$$

The equation (3.14) provides a phase correction to the periodic solution, which is a higher order correction to the condition $k^2 = q_c^2$ (3.10) consistent with the zero Lagrangian condition $L = 0$. From equation (3.14) we see that on an orbit with $\rho \rightarrow 0$ the equation for φ becomes singular unless the perturbed angular momentum vanishes. This is consistent with a heteroclinic connection to the zero solution, for which the perturbed angular momentum also vanishes. Integrating (3.14) with $M = 0$ in a neighbourhood of the fixed point on the heteroclinic orbit we have

$$\varphi = \frac{\delta^2}{\varepsilon} \frac{d\rho_0^2}{4(6k^2 - 2q_c^2)} X + \varphi_0, \quad (3.24)$$

where φ_0 is a constant, which we set equal to zero without loss of generality. Observe then that $\varphi = 0$ if $b_2 = d = 0$ in the symmetric case. Substituting $k = q_c$, $X = \varepsilon x$, (A.3), and (3.21) we have

$$\varphi = \delta^2 \frac{d\rho_0^2}{4(6k^2 - 2q_c^2)} x = q_c \frac{-9b_2^2\nu}{g\mu_2^2} x. \quad (3.25)$$

Thus, including this phase correction in the periodic solution $u(x)$ we get the correction for the wave number selection, so that

$$u(x, X) \sim \delta\rho(X)e^{ikx} + \text{c.c.} \quad (3.26)$$

$$k = q_c \left(1 - \frac{9b_2^2\nu}{\mu_2^2 g} \right). \quad (3.27)$$

Note that the phase correction φ is defined in terms of k , so that an approximation to the phase correction is obtained by setting $k = q_c$ in the definition of φ . Then we see that the phase correction is $O(\nu)$ in the asymmetric case. In the symmetric case, the coefficient $b_2 = 0$, so this correction vanishes. Then the phase correction is higher order; as shown in [15], the correction is $O(r^2)$ for $r \ll 1$.

As shown in [18], the result (3.27) is equivalent to setting $L = 0$ to this order of asymptotics. In the next section we compare the asymptotic results with the numerical calculation of the periodic solution with $H = L = 0$.

3.2 The symmetric nonlinearity: $b_2 = b_4 = 0$

The derivation of the amplitude equation follows the same procedure for the symmetric case. In that case, it is convenient to use a preliminary rescaling, $\hat{u} = |b_5|^{1/4}u$, so that the equation is, after dropping $\hat{\cdot}$'s,

$$u_t = - \left(q_c^2 + \frac{\partial^2}{\partial x^2} \right)^2 u + ru + \frac{b_3}{\sqrt{|b_5|}} u^3 + u^5. \quad (3.28)$$

Then the derivation proceeds as above. The expansion for u is given by

$$u(x, X) = \delta A_1(X) e^{ikx} + \delta^3 A_3(X) e^{3ikx} + \text{c.c.} + \dots, \quad (3.29)$$

noting that A_0 and A_2 vanish since they are proportional to b_2 and b_4 . Here ε is defined as before (2.12) and $\nu = b_3/\sqrt{|b_5|}$. Then the condition for a heteroclinic connection is given also by (3.20), which reduces in this case to

$$\varepsilon^2 |b_5| = b_3^2 \left(\frac{27}{160} + \frac{3\mu_1}{10\mu_3} \right). \quad (3.30)$$

In [15] this result was derived by using a different expansion, similar to that given in (2.9). In that case only the first term on the right hand side of (3.30) is obtained in the condition for the grain boundary corresponding to the localized oscillation. In practice, the second term on the right hand side of (3.30) is small, even though it is not related to any asymptotically small parameters, since $10\mu_3 > 600$. Then in the graph for the symmetric case in Section 4.1 we see little difference between the results obtained from the expansion (2.9) and those obtained from the expansion of this paper. This is discussed further following Figure 4.3.

As noted above, the correction in (3.27) to the leading order wave number $k = q_c$ vanishes in the symmetric case, since it is proportional to b_2 .

3.3 Stability of the localized rolls

As shown numerically in [11] and [12], the localized roll structure can be pinned or it may grow or shrink, depending on the choice of parameter values. One can view these variations as time and space dependent perturbations of the stationary envelope solution given in Section 3.1. To consider the effect of such perturbations we consider the time dependent amplitude equation, which can be derived as in the earlier part of this section by allowing the amplitude to vary on a slow time scale, $A = A(X, T)$ with $T = \varepsilon^2 t$. We consider the linear stability of the localized solutions in the context of the time-dependent amplitude equation,

$$\frac{\partial A}{\partial T} = (6k^2 - 2q_c^2) \frac{\partial^2 A}{\partial X^2} - A + 2|A|^2 A - c \frac{\delta^4}{\varepsilon^2} |A|^4 A. \quad (3.31)$$

This is the envelope equation for the symmetric case, which we consider first. We have also used the relationship between δ , ν and ε to simplify the coefficients.

Then, substituting

$$A(X) = [A_1(X) + \hat{\rho}(X, T)] e^{i\kappa(X, T)}, \quad (3.32)$$

into (3.31), where $A_1(X)$ satisfies (3.15), separating into real and imaginary parts, and keeping only the linear terms for $\hat{\rho} \ll 1$ and $\kappa \ll 1$ yields

$$\hat{\rho}_T = D\hat{\rho}_{XX} + \varepsilon^2\hat{\rho} - 2(3A_1^2(X))\hat{\rho} + 5c\frac{\delta^4}{\varepsilon^2}A_1^4\hat{\rho} \quad (3.33)$$

$$A_1\kappa_T = D(2\kappa_X A_1'(X) + \kappa_{XX}A_1(X)) \quad (3.34)$$

$$D = 6k^2 - 2q_c^2. \quad (3.35)$$

Assuming that $\hat{\rho} = A_1'(X)v(X)e^{\lambda_1 T}$ and $\kappa = K(X)e^{\lambda_2 T}$ and using the equation for A_1 , we find that

$$\lambda_2 A_1^2(X)K = D(A_1^2 K'(X))' \quad (3.36)$$

$$\lambda_1 (A_1'(X))^2 v = D((A_1'(X))^2 v'(X))'. \quad (3.37)$$

With appropriate conditions on $v(X)$ (for example, v vanishing for large $|X|$), and noting that the heteroclinic solution $A_1 > 0$ and is monotonic for finite X , we conclude that λ_1 and λ_2 are non-positive. Then we conclude that the localized solutions are stable to small perturbations, or that they are stable in a region of parameter space near the curve (3.20) which gives the condition for a heteroclinic connection. For the asymmetric case $b_2 \neq 0$, the same procedure can be used to study the linear stability of the modulus of the amplitude, replacing A_1 and c with ρ and g (3.16), respectively.

4 Numerical calculations.

4.1 Computation of the periodic solutions

In this section we compute the symmetric periodic solutions in x of the equation (1.1) which satisfy the periodic boundary conditions

$$u(0) = u(P), \quad u'(0) = u'(P),$$

where $P = 2\pi/k$ is an unknown.

There are many such periodic solutions. The ones of most interest to our calculations are those which are the limits of heteroclinic connections of solutions of (1.1) to the origin. Following the analysis of Section 3 these arise when the coefficients b_i are such that the periodic solution can simultaneously satisfy the conditions $H = L = 0$. To determine these periodic solutions we specify certain additional conditions. Firstly we fix the *phase* of the solution so that

$$u'(0) = u'(P) = 0.$$

Secondly we look only at solutions symmetric about $x = 0$ so that $u(x) = u(-x)$ and hence

$$u'''(0) = u'''(P) = 0.$$

It is certainly true that as the equation itself admits the symmetry $u \rightarrow u, \quad x \rightarrow -x$ there is a class of symmetric periodic solutions which bifurcate from zero at the critical value of $r = 0$ and which retain this symmetry. Thus it is not being overly restrictive to confine our attention to this class. For a general choice of coefficient values b_j we need

one additional condition to specify a periodic orbit. Two are of interest, the condition for a zero *Lagrangian* $L = 0$ solution (1.8), and secondly the condition for a zero *Hamiltonian* $H = 0$ defined by (1.9). These are chosen because a solution satisfying $L = 0$ corresponds to our earlier analysis and the condition $H = 0$ is necessary for a periodic solution to have a heteroclinic connection to the origin.

In principle, for a range of values of the coefficients b_j and r , then either of the two conditions $L = 0$ or $H = 0$ leads to a well defined periodic solution $u(x)$ together with an associated period P and frequency k . A path of such solutions as r varies may then be computed numerically. A simple procedure which works well for solutions satisfying $L = 0$ is firstly to guess values of $u(0)$, P and H . Using (1.9) we may then determine $u''(0)$. We have the further initial conditions $u'(0) = u'''(0) = 0$. We then integrate the system (1.1) with these initial conditions, together with the equation

$$\frac{dL}{dx} = -\frac{(u'')^2}{2} + 2q_c^2 \frac{(u')^2}{2} - (q_c^4 - r) \frac{u^2}{2} + F(u),$$

as an initial value problem over the interval $[0, P]$ using a variable order BDF method with error tolerance of 10^{-8} . Using the Powell-hybrid nonlinear solver SNSQE (see <http://gams.nist.gov/serve.cgi/Module/NMS/SNSQE/2828>), the values of $u(0)$, P and H are then adjusted until the three conditions

$$u(0) - u(P) = 0, \quad u'(P) = 0 \quad \text{and} \quad L(P) = 0 \quad (4.1)$$

are satisfied for the given value of r .

The procedure for finding solutions satisfying condition $H = 0$ is very similar but slightly simpler as in this case only $u(0)$ and P need to be determined. These procedures worked well given reasonable initial guesses. Having determined the solution at one value of r a branch of such solutions is then computed by using Keller's pseudo arc-length method [23].

When the solution satisfies $H = 0$ a careful use of bifurcation theory shows that there is a path of periodic solutions which bifurcates for $r < 0$ from the zero solution at the critical value of $r = 0$ [24]. This curve has a fold bifurcation at a point $r_1 < 0$ and exists for $r > r_1$.

In contrast the curve satisfying $L = 0$ does not bifurcate from the zero solution; however it does have a fold bifurcation precisely at the value $r = r_L$ corresponding to localized oscillatory solutions, where it *also* satisfies the condition $H = 0$ [18].

For a given value of r the procedure outlined above for finding the periodic solutions with $H = 0$ can be augmented to find the value of one of the coefficients b_j (together with P and $u(0)$) so that the condition $L = 0$ is also satisfied. This value of b_j is precisely the one at which we have a heteroclinic connection and its value can then be followed as r varies.

In Figure 4.1a we fix $q_c = 1$, $b_2 = 1$ and $b_3 = -0.5$ and present two numerically computed curves of k and H for periodic solutions (as a function of r) satisfying $L = 0$ for the case of the non-symmetric nonlinearity

$$f(u) = u^2 - \frac{1}{2}u^3.$$

Observe that the limit points in Figure 4.1a occur precisely when $H = 0$ and that at the left most limit point we also have $k \approx q_c$. The asymptotic approximation $k = q_c = 1$ for

the wave number for the localized pattern is shown by the dash-dotted line in Figure 4.1a. Note that this approximation is best precisely when $H = 0$.

In Figure 4.1b we extend this calculation. Keeping $b_2 = 1$ for each value of r we allow b_3 to vary so that $H = L = 0$. We then plot the value of the wavenumber k as a function of r . Observe that this is close to the value of $q_c(1 - 9b_2^2\nu/\mu_2^2g)$ from (3.27) for r close to 0, and deviates slowly from this value as $|r|$ increases.

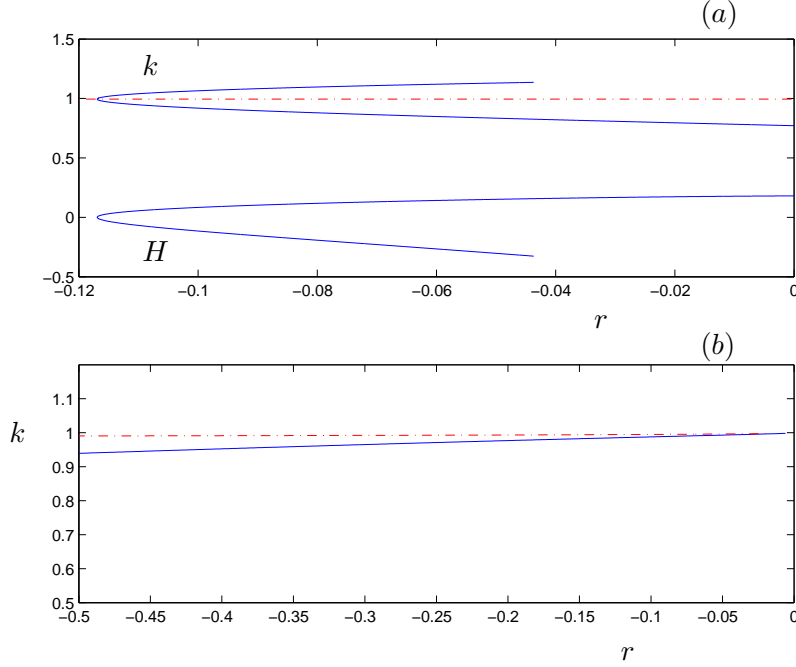


Figure 4.1: In the top graph (a) we show the numerical computations of H and k for the periodic solution with $L = 0$ and the asymmetric nonlinearity with $b_2 = 1$ and $b_3 = -0.5$. The dash-dotted line is the asymptotic approximation for the wave number (3.27). In the bottom graph (b) we compute a periodic solution with $H = L = 0$ and compare the wave number obtained analytically in (3.27) (solid line) with the wave number computed for the periodic solution with $H = L = 0$ (dash-dotted line).

4.2 Comparison of the numerical and asymptotic solutions

In this section we consider the parametric conditions for the heteroclinic connection. In particular we compare the asymptotic calculations of Section 3 (3.20) with the numerical computation of the special spatially periodic solution described above, which satisfies both $H = 0$ and $L = 0$. As shown in Section 3, the conditions for observing these periodic solutions correspond to the conditions for finding localized oscillations in (1.1).

In Figures 4.2-4.3 we show the numerically computed curves of (appropriate combinations of) coefficient values b_j as functions of r for which a periodic solution with $H = L = 0$ is found. We also compare these results with those obtained from the expansion (2.9), which is valid for $|r|$ near 0.

Figure 4.2 shows the results for the asymmetric case $b_2 \neq 0$. Taking $\tilde{u} = b_2 u$ in (1.1) the equation for \tilde{u} has coefficients of the quadratic and cubic terms given by 1 and b_3/b_2^2 , respectively. We conclude that b_3/b_2^2 is the appropriate parameter to use to represent

families of localized solutions, and this term is plotted as a function of r . In Figure 4.2, we see that the results from the asymptotic expansion of this paper, (3.20) (solid line) agree well with the numerical computation of the periodic solution with $L = 0$ and $H = 0$ (diamonds). Note that the r axis ranges from 0 to -2 . That is, the asymptotic results of Section 3 agree with the numerics for values of r and $O(1)$ distance from the bifurcation value of $r = 0$. In contrast, asymptotic results obtained from the expansion (2.9) are plotted as a dash-dotted line. As this expansion is based on the assumption that $|r| \ll 1$, these results fail for values of r away from zero. This difference in the range of applicability of the various expansions was also noted in [18] for the strut; there the difference of the results from (2.9) and (2.11) are also substantial for the asymmetric case, $b_2 \neq 0$.

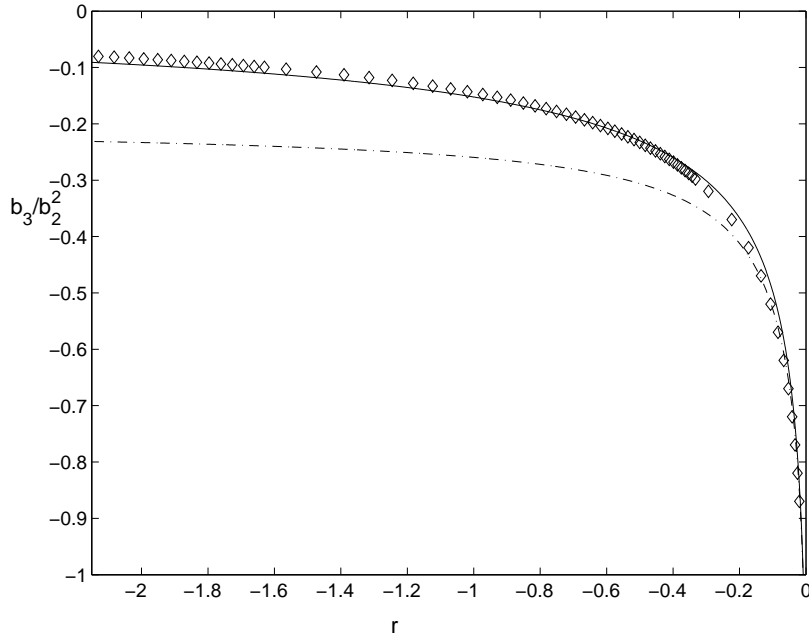


Figure 4.2: Graphs of the condition for the heteroclinic connection corresponding to localized solutions in the case of asymmetric nonlinearity, which can be expressed as a relationship between the bifurcation parameter r and the nonlinear coefficients b_j , in particular b_3/b_2^2 . The diamonds correspond to the solution obtained from the numerical calculation of periodic solutions satisfying $L = 0$ and $H = 0$, while the solid line gives the asymptotic results given by (3.20). The dash-dotted line gives the results obtained from using an expansion (2.9), valid for $|r|$ near 0.

In Figure 4.2 the results are shown for the particular case of $q_c = 1$. Through another rescaling we can get the results for the general case of $q_c \neq 1$ by setting $x \rightarrow x/q_c$, $u \rightarrow b_2/q_c^4 u$, the axes are transformed via,

$$r \rightarrow \frac{r}{q_c^4}, \quad \frac{b_3}{b_2^2} \rightarrow q_c^4 \frac{b_3}{b_2^2}. \quad (4.2)$$

In Figure 4.3 we show the results for the symmetric case $b_2 = b_4 = 0$. The graph is given in terms of r vs. the ratio $b_3/\sqrt{|b_5|}$, which reflects the rescaling $u = |b_5|^{-1/4} \hat{u}$, as in Section 3.2. Following this rescaling, the coefficients in the cubic and quintic terms in the equation for \hat{u} are just $b_3/\sqrt{|b_5|}$ and 1, respectively. In Figure 4.3 we again compare the results from (3.20) and (3.30) (solid line) with the numerical results (diamonds) and the results from the expansion (2.9). In this case all three curves are very close. For the

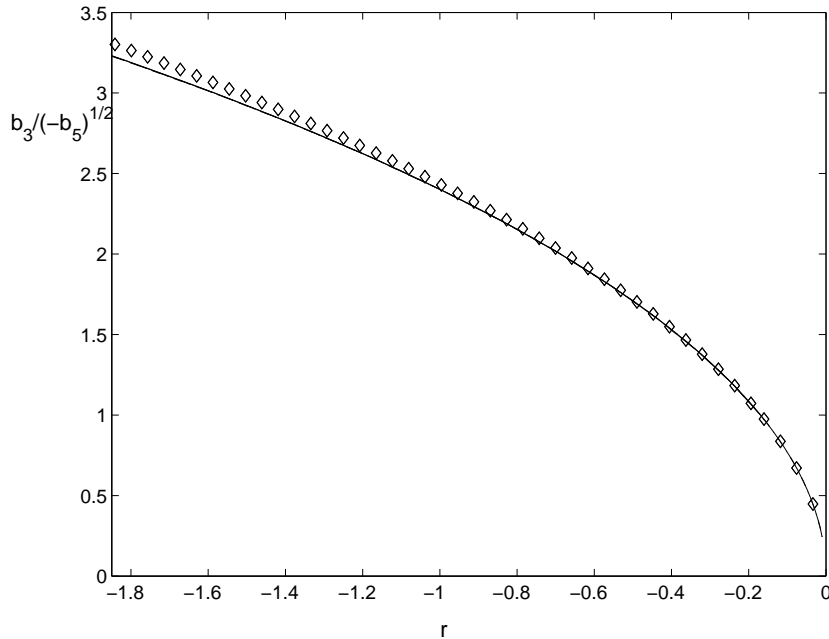


Figure 4.3: Graphs for the parameter values corresponding to the condition for localized solutions in the symmetric case. The diamonds correspond to the numerical solution while the solid gives the asymptotic results given by (3.20), (3.30). The dash-dotted line again gives the results from (2.9). In this case the solid and dash-dotted line are indistinguishable, since C_3 (3.11) is very small in practice.

case of the symmetric nonlinearity, the two expansions (2.11) and (2.9) lead to amplitude equations with different coefficients, but the actual values of the differences are small in practice; the difference arises through the terms involving C_3 in (3.11), which is small in practice (magnitude 10^{-2}).

In [18] a more significant difference was observed for localized buckling with the symmetric nonlinearity. In that setting the condition for the heteroclinic connection obtained from the approach of this paper were compared with the results from an expansion similar to (2.9), which was valid for parameter values near the bifurcation point. There the bifurcation parameter is the load \mathcal{P} , the coefficient of the second derivative in the equation. Then the small differences in the Swift-Hohenberg setting can be amplified in the strut model, due to the relationship between critical parameters in the models; for example, the bifurcation parameters for the two models are related through the nonlinear relationship $\mathcal{P} = 2q_c^2/\sqrt{q_c^4 - r}$.

5 Localized oscillations about non-zero steady states

For the asymmetric nonlinearity ($b_2 \neq 0$), we can also look for localized patterns described by connections or fronts between nonzero steady states and oscillatory patterns. In [12] localized structures of this type were computed numerically, primarily in the bistability regimes where both non-zero steady states and extended periodic solutions are stable. There the bifurcation structure of the steady and periodic solutions is given in detail, so we refer the reader to that discussion.

We use the analysis of Section 3 to give conditions for localized oscillations about $u = u_s$ where u_s is a non-zero steady state solution to (1.1); that is, we look for connections between u_s and oscillations about u_s . For simplicity of notation we demonstrate this for the case $b_2 \neq 0$, $b_3 \neq 0$ and $b_4 = b_5 = 0$. Then u_s satisfies

$$(r - q_c^4)u_s + b_2u_s^2 + b_3u_s^3 \Rightarrow u_s = \frac{1}{2b_3} \left[b_2 \pm (b_2^2 - 4b_3(r - q_c^4))^{1/2} \right]. \quad (5.1)$$

Oscillations about this steady state are then denoted $w = u - u_s$, which satisfies the equation

$$w_t = R w - \left(\frac{\partial^2}{\partial x^2} + q_c^2 \right) w + B_2 w^2 + B_3 w^3 \quad (5.2)$$

$$R = r + 2b_2u_s + 3b_3u_s^2, \quad B_2 = b_2 + 3b_3u_s, \quad B_3 = b_3. \quad (5.3)$$

We can repeat the analysis of Section 3 to look for localized oscillations for w , corresponding to connections between zero and the periodic solution. Replacing r and b_j with R and B_j , respectively, in the coefficients in (1.1), we construct the envelope for the oscillations, thus providing the condition (3.20) for localized oscillations in terms of R and B_j . Then this condition can be mapped from R and B_j back to the original parameters of the model, to yield conditions in terms of the original parameters for localized oscillations about non-zero steady states.

From the definition of u_s we see that these steady state solutions occur only if $(r - q_c^4) < \frac{b_2^2}{4b_3}$. Then it is convenient to write r and u_s as

$$r = q_c^4 + \alpha \frac{b_2^2}{4b_3}, \quad u_s = -\frac{b_2}{2b_3} \left[1 \pm \sqrt{1 - \alpha} \right]. \quad (5.4)$$

where $\alpha < 1$ for $b_3 < 0$. Substituting (5.4) into (5.3) yields

$$\begin{aligned} R &= r + \frac{b_2^2}{b_3} \left[\frac{3}{4} (1 \pm \sqrt{1 - \alpha})^2 - (1 \pm \sqrt{1 - \alpha}) \right] \equiv r + \frac{b_2^2}{b_3} g_1(\alpha), \\ \frac{B_3}{B_2^2} &= \frac{4b_3}{b_2^2} \frac{1}{(1 \pm 3\sqrt{1 - \alpha})^2} \equiv \frac{4b_3}{b_2^2} g_2(\alpha). \end{aligned} \quad (5.5)$$

The variables R and B_3/B_2^2 are convenient since they are analogous to those used in Figure 4.2 to graph the condition (3.20) for localized oscillations. That is, the condition for localized oscillations in the solution w is shown in Figure 4.2 if we replace the axes labels with R and B_3/B_2^2 . Then, through (5.5) and (5.4) we can map this curve back in terms of the original parameters, r and b_3/b_2^2 . We denote the values on the curve in Figure (4.2) as $(r_L(1), \mathcal{B}_L(1))$, with 1 denoting that $q_c = 1$ for these values. Then, for $q_c = 1$, the condition for w for a heterclinic connection between zero and periodic oscillations with $k \sim 1$ is found by setting $R = r_L(1)$ and $B_3/B_2^2 = \mathcal{B}_L(1)$. We also recall (4.2) which gives the transformation for a general q_c , to get

$$r_L(q_c) = q_c^4 r_L(1), \quad \mathcal{B}_L(q_c) = \frac{\mathcal{B}_L(1)}{q_c^4}. \quad (5.6)$$

Then, using (5.4) and (5.5), and setting $\mathcal{B}_L(1)/q_c^4 = \frac{B_3}{B_2^2}$ and $q_c^4 r_L(1) = R$, we have

$$\frac{b_3}{b_2^2} = \frac{\mathcal{B}_L(1)}{4q_c^4} g_2(\alpha), \quad \mathcal{B}_L(1)(r_L(1) - 1) = \frac{\alpha + 4g_1(\alpha)}{g_2(\alpha)}. \quad (5.7)$$

Using $\mathcal{B}_L(1)$ and $r_L(1)$ as determined in Section 3, together with (5.7) and (5.4), we find the condition for a heteroclinic connection between u_s and periodic oscillations about u_s , that is the condition for localized oscillations about a non-zero steady state. This condition is shown in terms of the parameters r and b_j in Figure 5.1, with the values of r obtained by varying α in the expressions above.

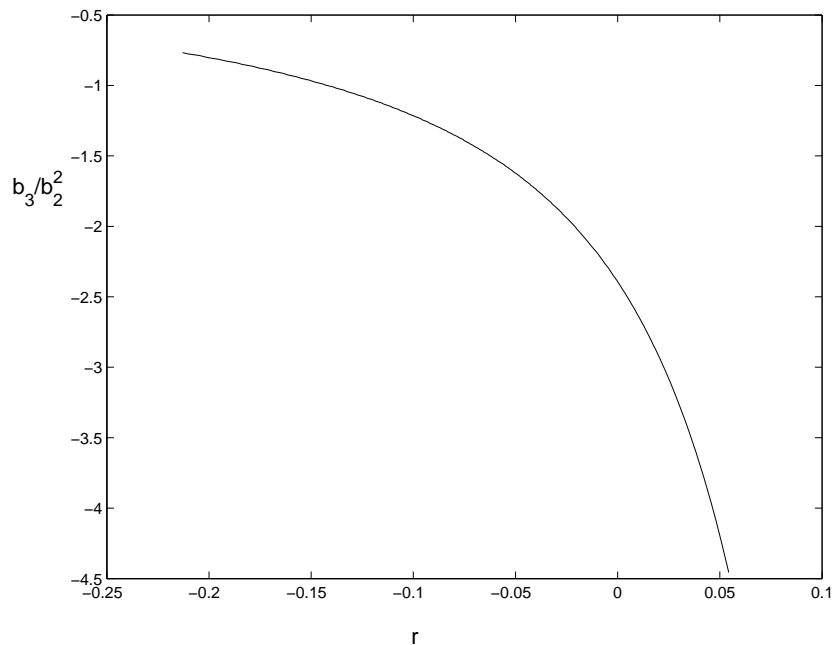


Figure 5.1: Graph for the parameter values corresponding to localized solutions with connection to non-zero steady state for the asymmetric case. Here we show the graph for the choice of the + sign in the definition of u_s in (5.4).

6 Discussion

In this paper we have presented a multiple scales analysis for constructing stationary localized cellular patterns for the generalized Swift-Hohenberg equation. The method provides an envelope equation for the amplitude of these patterns, from which we derive parametric conditions for connections or fronts between homogeneous and oscillatory solutions. The results presented here show the relation of the heteroclinic connection to the critical periodic orbit for which $L = H = 0$. We find that there is good agreement with numerical calculations of this special periodic solution, even far from the critical bifurcation values. The analysis also gives a correction to the wave number selection in the case of an asymmetric nonlinearity.

Calculation of the heteroclinic connection gives the mean parameter value at which we expect to see localized cellular patterns which can have an arbitrarily large number of rolls, as shown computationally in the symmetric case in [11] and discussed from a dynamical systems theory point of view in [17]. In fact, for each of the curves presented in Figs. 4.3 and 5.1 we expect to see an interval of parameter values, the width of which decreases exponentially as $r \rightarrow 0$, over which an arbitrary number of rolls is observed in the localized pattern. For parameter values outside of this interval, the localized solutions are no longer stationary, resulting in propagation of the fronts that connect the constant and cellular solutions [11] [17] [12]. In [11] an outline is given for a possible equation for this front propagation. The derivation of such an equation could also provide an analytical approximation for the interval in which the localized solutions are stable. The amplitude equation (3.12) obtained for the localized solution provides a starting point for this derivation.

A Appendix: Coefficients in the amplitude equation

In Section 3 we showed that

$$u_4 = R_4(X) + B_4(X)e^{2ikx} + D_4(X)e^{4ikx} + \text{c.c.}$$

The coefficients $R_4(X)$ and $B_4(X)$ are given by

$$\begin{aligned} \mu_2(k)B_2 &= b_2(2A_0B_2 + 2A_1^*C_3) - 4ib_2kA_2'(X) \frac{(-8k^2 + 2q_c^2)}{\mu_2} + 3b_3(2|A_1|^2B_2 + A_1^2A_0) + 4b_4A_1^2|A_1|^2 \\ \mu_0(k)B_0 &= b_2(2|B_2|^2 + A_0^2) + 3b_3(2|A_1|^2A_0 + A_1^2B_2^* + (A_1^*)^2B_2) + 6b_4|A_1|^4. \end{aligned} \quad (\text{A.1})$$

The coefficients c and d are given by

$$\begin{aligned} c &= -\frac{12b_2^4}{\mu_2^2\mu_3} - \frac{12b_2^2b_3}{\mu_2\mu_3} - \frac{6}{\mu_2^2} \left(\frac{2b_2^4}{\mu_0} + 3b_3b_2^2 \right) \\ &\quad - 4b_4 \left(\frac{6b_2}{\mu_2} + \frac{9b_2}{\mu_0} \right) - 10b_5 - \frac{36b_3b_2^2}{\mu_2\mu_0} - \frac{3b_3^2}{\mu_3} - 4 \left(2\frac{b_2^4}{\mu_0^3} + \frac{9b_3b_2^2}{\mu_0^2} \right) \end{aligned} \quad (\text{A.2})$$

$$d = \frac{32b_2^2k(q_c^2 - 4k^2)}{\mu_2^2}. \quad (\text{A.3})$$

We note that in the definition of c the terms of the form $1/\mu_3(k)$ and $1/\mu_2(k)^2$ are very small in comparison with the others.

References

- [1] G. Dewel, A. de Wit, B. Rudovics, J.J. Perraud, E. Dulos, J. Boissonade, J., P. de Kepper, “Pattern selection and localized structures in reaction-diffusion systems”, *Physica A*, **213**, 1995, p 181-98.
- [2] V. K. Vanag and I.R. Epstein, “Stationary and oscillatory localized patterns, and subcritical bifurcations” *Physical Review Letters* **92** 2004, 128301/1-4.
- [3] H. Riecke and G. D. Granzow, “Localization of waves without bistability: worms in nematic electroconvection” *Phys. Rev. Lett.* **81**, 1998, p 333-6.
- [4] Hartmann, N.; Kevrekidis, Y.; Imbihl, R. “Pattern formation in restricted geometries: The NO+CO reaction on Pt(100) *J. Chem. Phys.* **112**, 2000, p 6795-803.
- [5] Pattern formation, localized structures and solitons: strongly nonlinear structures in a self-organizing optical system T. Ackemann, E. Grofie-Westhoff, M.; Pesch, F.; Huneus, M.; Bolscher, W. Lange, *2003 Euro. Quant. Elect. Conf.* 2003, p 100.
- [6] A. R. Champneys, M.D. Grooves, and P.D. Woods, “A global characterization of gap solitary-wave solutions to a coupled KdV system, *Phys. Lett. A*, **271** (2000), 178-190.
- [7] G.W. Hunt, M.A. Peletier, A.R. Champneys, P.D. Woods, M. A. Wadee, C.J. Budd and G.L. Lord, *Cellular buckling in long structures*, *Nonlinear Dynamics*, **21**, (2000), 3–29.
- [8] W. Eckhaus and R. Kuske, “Pattern formation in systems with slowly varying geometry”, *SIAM J. Appl. Math.* **57** (1997), 112-152.
- [9] S. Setayeshgar, S. and M.C. Cross, “Turing instability in a boundary-fed system” *Phys Rev. E* **58** 1998, 4485-500.
- [10] Bar, M. I.G. Kevrekidis, H.-H. Rotermund, and G. Ertl, “Pattern formation in composite excitable media”, *Phys. Rev. E*, **52**, 1995, p R5739-42.
- [11] H. Sakaguchi and H. R. Brand, “Stable localized solutions of arbitrary length for the quintic Swift-Hohenberg equation”, *Physica D*, **97** (1990) 274-85.
- [12] M’F. Hilali, S. Metens, P. Borckmans, and G. Dewel, “Pattern selection in the generalized Swift-Hohenberg model”, *Phys. Rev. E*, **51**, 1995, 2046-52.
- [13] C. Crawford and H. Riecke, “Oscillon-type structures and their interaction in a Swift-Hohenberg model”, *Physica D*, **129** (1999), 83-92.
- [14] C. Bensimon, B. I. Shraiman, and V. Croquette, *Nonadiabatic effects in convection*, *Phys. Rev. A* **38** (1988), 5461–64.
- [15] A.A. Nepomnyaschy, M. I. Tribelsky, and M. G. Velarde, *Wave number selection in convection and related problems*, *Phys. Rev. E* **50** (1994) 1194–97.
- [16] Jensen, O. Pannbacker, V.O.; Mosekilde, E.; Dewel, G.; Borckmans, P. Localized structures and front propagation in the Lengyel-Epstein model *Phys. Rev. E* **50**, 1994, p 736-49.

- [17] P. Couillet, C. Riera, and C. Tresser, “Stable static localized structures in one dimension”, *Phys. Rev. Lett.* **84** 2000, 3069-3072.
- [18] C.J. Budd, G. W. Hunt, and R. Kuske, “ Asymptotics of cellular buckling close to the Maxwell load”, *Proc. Royal Soc.*, **457** 2001, 2935-2964.
- [19] Y. Pomeau, ‘Front motion, metastability and subcritical bifurcations in hydrodynamics”, *Physica D* **23** 1986, 3-11.
- [20] P. Manneville, *Dissipative Structures and Weak Turbulence*, (1990), Academic Press, San Diego.
- [21] L. Yu Glesky and L.M. Lerman,“ On small stationary localized solutions for the generalized 1-D Swift-Hohenberg equation”, *Chaos* **5**1995, 424-431.
- [22] Belyakov, L. A.; Glebsky, L. Yu.; Lerman, L. M., “Abundance of stable stationary localized solutions to the generalized 1D Swift-Hohenberg equation” *Comput. Math. Appl.* **34** (1997), 253–266.
- [23] H. Keller, *Numerical methods for two-point boundary value problems*, SIAM, 1976, Dover (reprint) 1996.
- [24] R. Beardmore, M. Peletier, C. Budd and A. Wadee, ‘Bifurcations of periodic solutions satisfying the zero-Hamiltonian constraint in reversible differential equations”, *SIAM J. Math. Analysis* **36** (2005), 1461-1488